Bioorganic & Medicinal Chemistry 19 (2011) 4513–4519

Contents lists available at ScienceDirect

Bioorganic & Medicinal Chemistry

journal homepage: www.elsevier.com/locate/bmc

Synthesis, molecular modeling and biological evaluation of β-ketoacyl-acyl carrier protein synthase III (FabH) as novel antibacterial agents

Hong-Jia Zhang, Di-Di Zhu, Zi-Lin Li, Juan Sun, Hai-Liang Zhu *

State Key Laboratory of Pharmaceutical Biotechnology, Nanjing University, Nanjing 210093, PR China

ARTICLE INFO

Article history:
Received 20 April 2011
Revised 5 June 2011
Accepted 8 June 2011
Available online 6 July 2011

Keywords:
Cinnamic acid
Secnidazole
Antibacterial activity
FabH inhibitors

ABSTRACT

A series of novel cinnamic acid secnidazole ester derivatives have been designed and synthesized, and their biological activities were also evaluated as potential inhibitors of FabH. These compounds were assayed for antibacterial activity against *Escherichia coli*, *Pseudomonas aeruginosa*, *Bacillus subtilis* and *Staphylococcus aureus*. Compounds with potent antibacterial activities were tested for their *E. coli* FabH inhibitory activity. Compound **3n** showed the most potent antibacterial activity with MIC of 1.56–6.25 μg/mL against the tested bacterial strains and exhibited the most potent *E. coli* FabH inhibitory activity with IC_{50} of 2.5 μM. Docking simulation was performed to position compound **3n** into the *E. coli* FabH active site to determine the probable binding conformation.

1. Introduction

Although several classes of antibacterial agents are presently available, resistance in most of the pathogenic bacteria to these drugs constantly emerges. In order to prevent this serious medical problem, the elaboration of new types of antibacterial agents is a very important task.[1] Recent 10 years, different targets in key areas of the bacterial cell cycle have been studied that would be a new weapon against the problem of acquired resistance. One of the most attractive biochemical pathways to be used as the target for new antibacterial agents is the fatty acid biosynthesis (FAS). This pathway has been demonstrated to be essential for bacteria cell survival, and differs considerably from human FAS pathway.[2,3] While in humans fatty acid synthesis occurs in a homodimeric multifunctional enzyme,[4] in bacteria the pathway is composed of various discrete enzymes and each one can be considered a putative molecular target. Those features make the type II FAS pathway a potential target for new antimicrobial agents.

A key enzyme in this pathway is the β-ketoacyl-acyl carrier protein synthase III (FabH), which is the enzyme responsible for the first reaction in the pathway and plays an important regulatory role.[5] FabH has also been demonstrated to be essential for organismal survival and is present in a large number of important human pathogens.[6] Further more, some chemical compounds had shown to inhibit FabH from diverse microorganisms, including multi-drug resistant strains.[7,8] These facts support the idea that FabH can be used as an effective molecular target for the development of new antimicrobial agents.

Nitroimidazoles have been extensively used as antimicrobial chemotherapeutics and as antiangiogenic hypoxic cell radiosensitizers.[9] Nitroimidazole derivatives have attracted considerable attention as they can undergo bioreduction to yield electrophilic substances which can damage protein and nucleic acids.[10] Importantly, the toxicology and metabolism of nitroimidazoles, particularly secnidazole, have been characterized. Secnidazole (α,2-dimethyl-5-nitro-1*H*-imidazole-1-ethanol) is used as an antiprotozoal, antiamebic, and antibacterial drug.[11] It is an antimicrobic agent which is structurally related to the commonly used 5-nitromidazoles metronidazole and tinidazole. Secnidazole is particularly effective in the treatment of amebiasis, giardiasis, trichomoniasis, and bacterial vaginosis[12] as it is rapidly and completely absorbed after oral administration and has a longer terminal elimination half-life (17–29 h) than commonly used drugs in this class.[13] In these cases, the treatment with secnidazole is shorter and significantly more effective than the treatment using other imidazole drugs and the adverse effects are not very drastic.[14] As a result, excellent reviews have been published on the activity and pharmacokinetics of secnidazole and their determination in pharmaceutical is of great importance.

As apart of our research for novel antibacterial agents, we designed and synthesized a series of secnidazole analogs based on cinnamic acid scaffold. We chose cinnamoyl moiety as it was found in a variety of biologically active substances.[15,16] Antibacterial activities of various cinnamic acid derivatives were also explored by many research groups.[17] Particularly, cinnamic acid ester derivatives showed the potential antibacterial activity.[18] However,

* Corresponding author. Tel.: +86 25 8359 2572; fax: +86 25 8359 2672.
E-mail address: zhuhl@nju.edu.cn (H.-L. Zhu).

0968-0896/$ - see front matter Crown Copyright © 2011 Published by Elsevier Ltd. All rights reserved.
doi:10.1016/j.bmc.2011.06.021

to our knowledge, few reports have been dedicated to the synthesis and FabH inhibitory activity of cinnamic acid secnidazole ester derivatives. In continuation to extend our research on the activity of cinnamic acid nitroimidazole ester derivatives, we report in the present work the synthesis and structure–activity relationships of a series of secnidazole derivatives.[19] Herein, we described the synthesis and the SAR of the novel series of secnidazole derivatives, and the biological activity evaluation indicated that some of these compounds are potent inhibitors of *Escherichia coli* FabH. Docking simulations were also performed using the X-ray crystallographic structure of the *E. coli* FabH with an inhibitor to explore the binding models of these compounds at the active site.

2. Results and discussion

2.1. Chemistry

The synthetic route for the novel cinnamic acid secnidazole ester derivatives **3a–t** is outlined in Scheme 1. These compounds were synthesized from the start cinnamic acids (**1**) and secnidazole

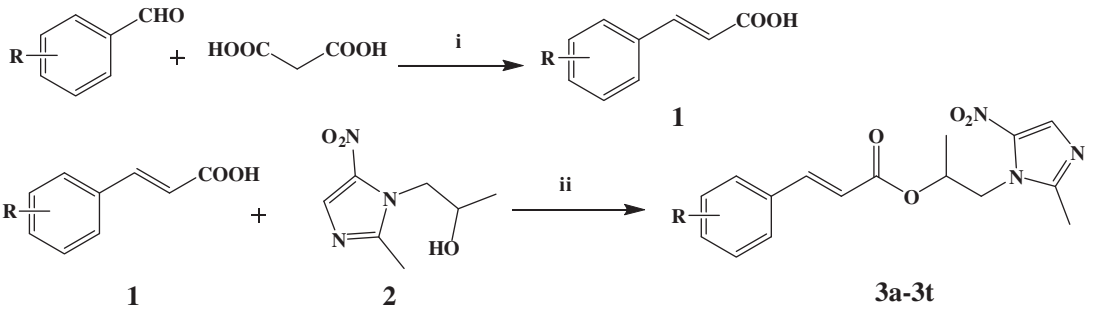

Scheme 1. General synthesis of cinnamic acid secnidazole ester derivatives (**3a–t**). Reagents and conditions: (i) piperidine, pyridine, 80–90 °C, 24 h; (ii) DCC, DMAP, 50–60 °C, 24 h.

Table 1
Structure of cinnamic acid secnidazole ester derivatives (**3a–t**)

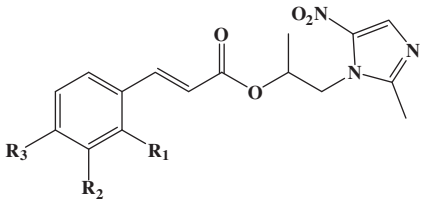

Compound	R_1	R_2	R_3
3a	H	H	H
3b	F	H	H
3c	Cl	H	H
3d	Br	H	H
3e	OCH_3	H	H
3f	H	F	H
3g	H	Br	H
3h	H	OCH_3	H
3i	H	H	F
3j	H	H	Cl
3k	H	H	Br
3l	H	H	CH_3
3m	H	H	OCH_3
3n	H	H	Ph
3o	H	H	OBn
3p	H	H	$N(CH_3)_2$
3q	Cl	H	Cl
3r	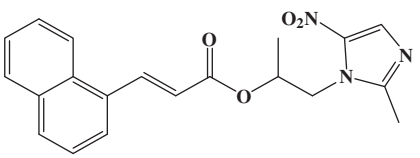	**3s**	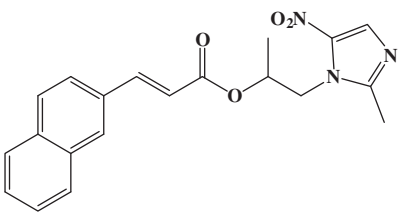
3t	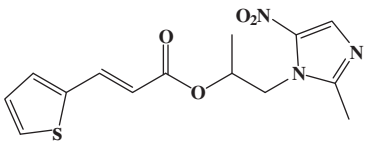		

(**2**). Compound (**1**) was prepared according the modified procedure of Davis et al.[20] Aromatic aldehydes and malonic acid were dissolved in a mixture of pyridine and piperidine and refluxed for 24 h, and cinnamic acids were obtained with yields of 75–85%. Then, cinnamic acids (**1**), secnidazole (**2**) and K_2CO_3 were taken in DMF and refluxed to obtain the desired compounds (**3a–t**) (Table 1). All of the synthetic compounds gave satisfactory analytical and spectroscopic data, which were in full accordance with their depicted structures.

2.2. Biological activity

2.2.1. Antibacterial activity

All the synthesized compounds were screened for antibacterial activity against two Gram-negative bacterial strains: *E. coli* and *Pseudomonas aeruginosa* and two Gram-positive bacterial strains: *Bacillus subtilis* and *Staphylococcus aureus* by MTT method. The MICs (minimum inhibitory concentrations) of the compounds against these bacteria were presented in Table 2. Also included was the activity of reference compound Kanamycin. The results revealed that most of the synthesized compounds exhibited significant antibacterial activities.

Out of the 20 synthetic new ester derivatives, compound **3n**, (*E*)-1-(2-methyl-5-nitro-1*H*-imidazol-1-yl)propan-2-yl 3-(biphenyl-4-yl)acrylate, exhibited the most potent antibacterial activity with MIC of 1.56, 3.13, 6.25, and 1.56 μg/mL against *E. coli*, *P. aeruginosa*, *B. subtilis* and *S. aureus*, respectively, which was similar to the broad-spectrum antibiotic Kanamycin with corresponding MIC of 3.13, 3.13, 1.56, and 1.56 μg/mL. Structure–activity relationships in these cinnamic acid secnidazole ester derivatives demonstrated that compounds with substitution at the *meta* (**3f–h**) or *para* (**3i–p**) position showed more potent activities than those with substitution at the *ortho* position (**3b–e**). A comparison of the *para* position substitution on benzene ring demonstrated that a *para* halogen group (**3i–k**) may have more slightly improved antibacterial activity and the potency order is F < Cl < Br, and other *para* substituents prepared (**3n–q**) had outstanding effect compared with **3a**, especially compound **3n** showed the best biological activity with MIC of 1.56 μg/mL against *E. coli*, which was superior to the positive control Kanamycin. However, a methyl or methoxy group substituent (**3l** and **3m**) led to a great loss of activity. Meanwhile, a significant loss of activity was observed when the chlorine group substituent was removed from the *para* position, compared with **3c**, which had one single chlorine group substituent at the *ortho* position. When the benzene ring was replaced by naphthalene or thiophene ring, a significant loss of activity was observed. Based on the data obtained from compounds with bromine group substituent (**3d**, **3g**, **3k**), we found that the potency order of antibacterial activity was *para* > *meta* > *ortho*.

Table 2
Antibacterial activity of synthetic compounds

Compounds	Minimum inhibitory concentrations (μg/mL)			
	Gram-negative		Gram-positive	
	E. coli ATCC35218	*P. aeruginosa* ATCC13525	*B. subtilis* ATCC 6633	*S. aureus* ATCC 6538
3a	>100	>100	>100	>100
3b	>100	>100	>100	>100
3c	50	25	50	50
3d	25	25	50	25
3e	>100	>100	>100	>100
3f	3.13	3.13	6.25	6.25
3g	12.5	12.5	25	12.5
3h	>100	>100	>100	>100
3i	50	50	50	100
3j	12.5	25	12.5	25
3k	6.25	6.25	3.13	3.13
3l	100	50	>100	>100
3m	>100	>100	50	50
3n	1.56	3.13	6.25	1.56
3o	3.13	6.25	6.25	3.13
3p	6.25	6.25	12.5	6.25
3q	3.13	6.25	6.25	12.5
3r	25	50	25	50
3s	50	50	50	100
3t	50	50	>100	50
Kanamycin	3.13	3.13	1.56	1.56

2.2.2. *E. coli* FabH inhibitory activity

The *E. coli* FabH inhibitory potency of the synthetic ester derivatives with potent antibacterial activities (**3d**, **3f**, **3g**, **3j**, **3k**, **3p**–**r**) was examined and the results are summarized in Table 3. Most of the tested compounds displayed potent *E. coli* FabH inhibitory. Among them, compound **3n** condensing by (*E*)-3-(biphenyl-4-yl)acrylic acid and secnidazole showed the most potent inhibitory with IC_{50} of 2.5 μM. This result supported the potent antibacterial activities of **3n**. Compound **3o** which with similar structure to **3n** exhibited good inhibitory with MIC of 6.7 μM. Other tested compounds displayed moderate inhibitory activity with MIC ranging from 8.2 to 48.9 μM. Compound **3k** with *p*-substituted bromine group on cinnamic acid component showed better *E. coli* FabH inhibitory activity than compounds **3d** and **3g** with *o*-substituted and *m*-substituted bromine group. Compound **3q** with both *o*-substituted and *p*-substituted chloro groups showed more preferable inhibitory activity than compound **3j** with single *p*-substituted chloro group. In addition, the inhibitory activity of compound **3r** condensing by (*E*)-3-(naphthalen-1-yl)acrylic acid and secnidazole was obviously decreased.

The results of *E. coli* FabH inhibitory activity of the test compounds were corresponding to the structure relationships (SAR) of their antibacterial activities. This demonstrated that the potent antibacterial activities of the synthetic compounds were probably correlated to their FabH inhibitory activities.

2.3. Molecular docking study of synthetic compounds and binding model of compound 3n and *E. coli* FabH

The binding affinity was evaluated by binding energy and inhibitory constant. Molecular docking of all the synthesized compounds and *E. coli* FabH was performed on the binding model based on the *E. coli* FabH-CoA complex structure (1HNJ.pdb).[21] The FabH active site generally contains a catalytic triad tunnel consisting of Cys-His-Asn, which is conserved in various bacteria. This catalytic triad plays an important role in the regulation of chain elongation and substrate binding. Since the alkyl chain of CoA is broken by Cys of the catalytic triad of FabH, interactions between Cys and substrate appear to play an important role in substrate

Table 3
E. coli FabH inhibitory activity of synthetic compounds

Compounds	*E. coli* FabH IC_{50} (μM)	Hemolysis LC (mg/mL)
3d	40.1	>10
3f	8.2	>10
3g	27.5	>10
3j	34.3	>10
3k	15.6	>10
3n	2.5	>10
3o	6.7	>10
3p	19.8	>10
3q	9.4	>10
3r	48.9	>10
Secnidazole	28.5	>10
Cinnamic acid	43.4	>10

binding. Qiu et al. have refined three-dimensional structure of *E. coli* FabH in the presence and absence of malonyl-CoA by X-ray spectroscopy. Since malonyl moiety is degraded by *E. coli* FabH, molecular docking studies for FabH and malonyl-CoA was carried out to identify a plausible malonyl-binding model.[21] They found that in one of the binding modes appeared in the lower scored conformations, the malonyl carboxylate formed hydrogen bonds to the backbone nitrogen of Phe 304.

The binding affinity of the synthesized compounds and *E. coli* FabH is depicted in Table 4. As shown in Table 4, the results of binding energy and inhibitory constant have the same trend. Structure–activity relationships in compounds **3a–t** demonstrated that compounds with different substituent group exhibit different parameter. Among them, compound **3n** with *p*-substituted phenyl group showed minimum data, which suggested that this compound was mostly easy to combine with *E. coli* FabH. The selected pose of compound **3n** had an estimated free energy of binding of −20.2 kcal/mol and inhibitory constant of 1.56 fm. The estimated free energy of other compounds (**3a–m**, **3o–t**) are ranging from −19.1 to −15.78 kcal/mol and inhibitory constants are ranging from 10.01 fm to 2.73 pm, respectively. This molecular docking result, along with the biological assay data, suggesting that compound **3n** is a potential inhibitor of *E. coli* FabH.

Table 4
Docking parameters of synthetic compounds

Compounds	Binding energy ΔGb (kcal/mol)	Inhibitory constant
3a	−16.2	1.32 pm
3b	−16.39	974.95 fm
3c	−17.99	65.24 fm
3d	−16.75	528.96 fm
3e	−16.03	1.79 pm
3f	−18.38	33.61 fm
3g	−17.28	214.08 fm
3h	−15.78	2.73 pm
3i	−17.43	168.56 fm
3j	−18.0	63.96 fm
3k	−17.87	79.87 fm
3l	−16.44	895.78 fm
3m	−16.66	609.79 fm
3n	−20.2	1.56 fm
3o	−19.1	10.01 fm
3p	−17.67	111.2 fm
3q	−18.53	26.14 fm
3r	−16.85	443.44 fm
3s	−16.75	525.58 fm
3t	−16.72	555.12 fm

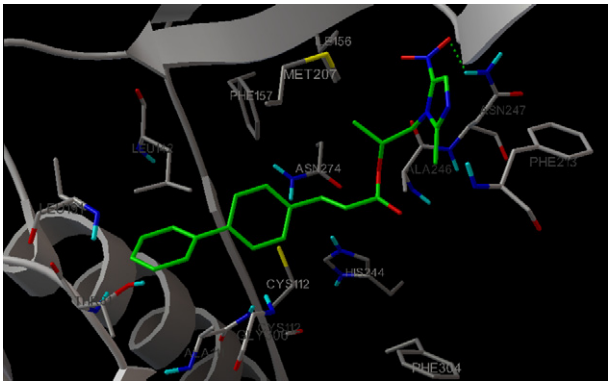

Figure 1. (A) Binding model of compound **3n** (colored in green) into *E. coli* FabH. H-bond is shown as dotted green lines. Asn247 forms hydrogen bond with the oxygen atom of the nitro group of compound **3n**. (B) 3D model of the interaction between compound **3n** and the colchicine binding site. The protein is represented by molecular surface. Compound **3n** is depicted by sticks and balls.

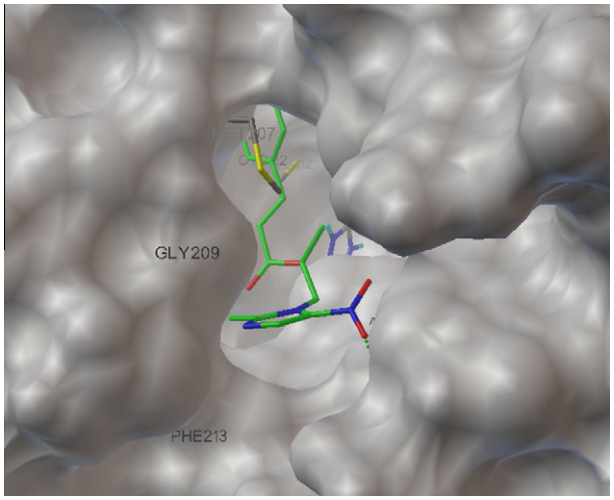

Fig. 1 (*continued*)

Compound **3n** which displayed the most potent *E. coli* FabH inhibitory activity was selected for further molecular docking study. The binding model of compound **3n** and *E. coli* FabH is depicted in Figure 1. It can be seen from Figure 1 that, in the binding model of compound **3n** and *E. coli* FabH, there is one hydrogen bond. Asn247 froms hydrogen bond with the oxygen atom of the nitro group of compound **3n**. The result along with the data of *E. coli* FabH inhibitory activity assay indicated that compound **3n** would be potential inhibitors of *E. coli* FabH with potent antibacterial activity.

3. Conclusions

A series of novel ester derivatives reacting by cinnamic acid and secnidazole were synthesized and assayed for their antibacterial activities against *E. coli*, *P. aeruginosa*, *B. subtilis* and *S. aureus*. Compound **3n**, (*E*)-1-(2-methyl-5-nitro-1*H*-imidazol-1-yl)propan-2-yl 3-(biphenyl-4-yl)acrylate showed the most potent antibacterial activity with MIC of 1.56–6.25 μg/mL against the test bacterial strains and exhibited the most potent *E. coli* FabH inhibitory activity with IC_{50} of 2.5 μM, which was compared with the positive control Kanamycin. Docking simulation was performed to position compound **3n** into the *E. coli* FabH active site to determine the probable binding conformation. Analysis of the compound **3n**'s binding conformation in active site displayed the compound **3n** was stabilized by hydrogen bonding interactions with Asn247. Antibacterial assay results also showed that these cinnamic acid secnidazole ester derivatives had the potential to be developed for antibacterial agents against *E. coli*. Particularly, compound **3n** has demonstrated significant *E. coli* FabH inhibitory activity as a potential antibacterial agent.

4. Experiments

4.1. Materials and measurements

All chemicals and reagents used in current study were analytical grade. All the ^{1}H NMR spectra were recorded on a Bruker DPX 300 model Spectrometer in DMSO–d_6 and chemical shifts were reported in ppm (δ). ESI-MS spectra were recorded on a Mariner System 5304 Mass spectrometer. Elemental analyses were performed on a CHN-O-Rapid instrument. TLC was performed on the glass-backed silica gel sheets (silica gel 60 Å GF254) and visualized in UV light (254 nm).

4.2. General procedure for synthesis of cinnamic acids

A mixture of aromatic aldehydes (3.2 mmol), malonic acid (3.87 mmol), piperidine (0.387 mmol) was dissolved in pyridine and stirred on 80–90 °C for 24 h. The pyridine was removed at the vacuum. The reaction mixture was poured in water and washed with HCl, the precipitate was filtered and washed with hexane about three times, and dried under vacuum to afford the cinnamic acids (Scheme 1)

4.3. General procedure for synthesis of cinnamic acid secnidazole ester derivatives

Equimolar amount of secnidazole (1.0 mmol) and cinnamic acid (1.0 mmol) were dissolved in dichloromethane, DCC (1.5 mmol) and DMAP (0.5 mmol) as catalyst and stirred at 50–60 °C for 24 h. The reaction mixture was extracted with ethyl acetate and saturated sodium bicarbonate, respectively. Then, the organic layer was collected and crystallized to get the product (Scheme 1).

4.3.1. (*E*)-1-(2-Methyl-5-nitro-1*H*-imidazol-1-yl)propan-2-yl cinnamate (3a)

Light grey powder, yield 60.9%, mp: 136–139 °C, ^{1}H NMR (300 MHz, $CDCl_3$, δ ppm): 1.42 (d, J = 4.62 Hz, 3H), 2.49 (s, 3H), 3.76–3.78 (m, 1H), 4.10–4.14 (m, 2H), 6.75 (d, J = 9.24 Hz, 1H), 7.02 (s, 1H), 7.37–7.39 (m, 3H), 7.48–7.50 (m, 2H), 7.67 (s, 1H). ESI-MS: 316.1 ($C_{16}H_{18}N_3O_4$, $[M+H]^+$). Anal. Calcd for $C_{16}H_{17}N_3O_4$: C, 60.94; H, 5.43; N, 13.33. Found: C, 60.67; H, 5.56; N, 13.45.

4.3.2. (*E*)-1-(2-Methyl-5-nitro-1*H*-imidazol-1-yl)propan-2-yl 3-(2-fluorophenyl)acrylate (3b)

White powder, yield 65.6%, mp: 106–107 °C, ^{1}H NMR (300 MHz, $CDCl_3$, δ ppm): 1.42 (d, J = 4.62 Hz, 3H), 2.54 (s, 3H), 4.29–4.37 (m, 1H), 4.64–4.71 (m, 1H), 5.38–5.43 (m, 1H), 6.39 (d, J = 16.08 Hz, 1H), 7.08–7.19 (m, 2H), 7.34–7.41 (m, 1H), 7.49 (t, J = 7.50 Hz, 1H), 7.71 (d, J = 16.26 Hz, 1H), 7.93 (s, 1H). ESI-MS: 334.1 ($C_{16}H_{17}FN_3O_4$, $[M+H]^+$). Anal. Calcd for $C_{16}H_{16}FN_3O_4$: C, 57.65; H, 4.84; N, 12.61. Found: C, 57.67; H, 4.87; N, 12.77.

4.3.3. (*E*)-1-(2-Methyl-5-nitro-1*H*-imidazol-1-yl)propan-2-yl 3-(2-chlorophenyl)acrylate (3c)

White powder, yield 61.1%, mp: 125–127 °C, ^{1}H NMR (300 MHz, $CDCl_3$, δ ppm): 1.44 (d, J = 6.42 Hz, 3H), 2.55 (s, 3H), 4.30–4.38 (m, 1H), 4.64–4.70 (m, 1H), 5.38–5.43 (m, 1H), 6.27 (d, J = 16.08 Hz, 1H), 7.25–7.35 (m, 2H), 7.40–7.43 (m, 1H), 7.55–7.58 (m, 1H), 7.93 (s, 1H), 8.00 (d, J = 16.08 Hz, 1H). ESI-MS: 350.1 ($C_{16}H_{17}ClN_3O_4$, $[M+H]^+$). Anal. Calcd for $C_{16}H_{16}ClN_3O_4$: C, 54.94; H, 4.61; N, 12.01. Found: C, 54.69; H, 4.81; N, 12.45.

4.3.4. (*E*)-1-(2-Methyl-5-nitro-1*H*-imidazol-1-yl)propan-2-yl 3-(2-bromophenyl)acrylate (3d)

White powder, yield 57.0%, mp: 112–115 °C, ^{1}H NMR (300 MHz, $CDCl_3$, δ ppm): 1.44 (d, J = 6.39 Hz, 3H), 2.55 (s, 3H), 4.09 (d, J = 8.40 Hz, 1H), 4.30–4.38 (m, 1H), 4.64–4.70 (m, 1H), 5.36–5.44 (m, 1H), 6.23 (d, J = 15.99 Hz, 1H), 7.21–7.26 (m, 1H), 7.33 (t, J = 7.13 Hz, 1H), 7.54–7.57 (m, 1H), 7.59–7.62 (m, 1H), 7.93 (s, 1H). ESI-MS: 394.0 ($C_{16}H_{17}BrN_3O_4$, $[M+H]^+$). Anal. Calcd for $C_{16}H_{16}BrN_3O_4$: C, 48.75; H, 4.09; N, 10.66. Found: C, 48.61; H, 4.51; N, 11.15.

4.3.5. (*E*)-1-(2-Methyl-5-nitro-1*H*-imidazol-1-yl)propan-2-yl 3-(2-methoxyphenyl)acrylate (3e)

White powder, yield 59.2%, mp: 158–162 °C, ^{1}H NMR (300 MHz, $CDCl_3$, δ ppm): 1.59 (d, J = 7.21 Hz, 3H), 1.98 (s, 3H), 3.76–3.80 (m, 1H), 3.84 (s, 3H), 4.03–4.17 (m, 2H), 6.75 (d, J = 15.36 Hz, 1H), 6.92–6.96 (m, 2H), 7.02 (s, 1H), 7.10 (d, J = 7.68 Hz, 1H), 7.28–7.34 (m, 1H), 7.66 (d, J = 15.36 Hz, 1H). ESI-MS: 346.1 ($C_{17}H_{20}N_3O_5$, $[M+H]^+$). Anal. Calcd for $C_{17}H_{19}N_3O_5$: C, 59.12; H, 5.55; N, 12.17. Found: C, 58.81; H, 5.75; N, 11.95.

4.3.6. (*E*)-1-(2-Methyl-5-nitro-1*H*-imidazol-1-yl)propan-2-yl 3-(3-fluorophenyl)acrylate (3f)

White powder, yield 66.2%, mp: 133–136 °C, ^{1}H NMR (300 MHz, $CDCl_3$, δ ppm): 1.41 (d, J = 7.09 Hz, 3H), 2.42 (s, 3H), 4.13–4.18 (m, 1H), 4.34–4.36 (m, 1H), 4.61–4.66 (m, 1H), 6.56 (d, J = 15.36 Hz, 1H), 7.24–7.26 (m, 1H), 7.39 (d, J = 8.24 Hz, 1H), 7.56 (t, J = 6.93 Hz, 2H), 7.71 (s, 1H), 7.97 (s, 1H). ESI-MS: 334.1 ($C_{16}H_{17}FN_3O_4$, $[M+H]^+$). Anal. Calcd for $C_{16}H_{16}FN_3O_4$: C, 57.65; H, 4.84; N, 12.61. Found: C, 58.05; H, 4.62; N, 12.34.

4.3.7. (*E*)-1-(2-Methyl-5-nitro-1*H*-imidazol-1-yl)propan-2-yl 3-(3-bromophenyl)acrylate (3g)

Light yellow powder, yield 67.2%, mp: 102–104 °C, ^{1}H NMR (300 MHz, $CDCl_3$, δ ppm): 1.43 (d, J = 6.57 Hz, 3H), 2.54 (s, 3H), 4.09–4.16 (m, 1H), 4.32–4.40 (m, 1H), 4.63–4.69 (m, 1H), 6.27 (d, J = 15.90 Hz, 1H), 7.26 (t, J = 7.86 Hz, 1H), 7.41 (d, J = 7.68 Hz, 1H), 7.51 (t, J = 7.97 Hz, 2H), 7.64 (s, 1H), 7.94 (s, 1H). ESI-MS: 394.0 ($C_{16}H_{17}BrN_3O_4$, $[M+H]^+$). Anal. Calcd for $C_{16}H_{16}BrN_3O_4$: C, 48.75; H, 4.09; N, 10.66. Found: C, 48.89; H, 3.98; N, 11.12.

4.3.8. (*E*)-1-(2-Methyl-5-nitro-1*H*-imidazol-1-yl)propan-2-yl 3-(3-methoxyphenyl)acrylate (3h)

White powder, yield 72.9%, mp: 148–151 °C, ^{1}H NMR (300 MHz, $CDCl_3$, δ ppm): 1.42 (d, J = 6.66 Hz, 3H), 2.40 (s, 3H), 3.82 (s, 3H), 4.04 (d, J = 7.50 Hz, 2H), 4.12–4.16 (m, 1H), 6.73 (d, J = 15.39 Hz, 1H), 6.91–6.94 (m, 2H), 7.00 (s, 1H), 7.09 (d, J = 7.50 Hz, 1H), 7.26–7.33 (m, 1H), 7.64 (d, J = 15.36 Hz, 1H). ESI-MS: 346.1 ($C_{17}H_{20}N_3O_5$, $[M+H]^+$). Anal. Calcd for $C_{17}H_{19}N_3O_5$: C, 59.12; H, 5.55; N, 12.17. Found: C, 59.33; H, 4.98; N, 12.52.

4.3.9. (*E*)-1-(2-Methyl-5-nitro-1*H*-imidazol-1-yl)propan-2-yl 3-(4-fluorophenyl)acrylate (3i)

White powder, yield 66.7%, mp: 145–147 °C, ^{1}H NMR (300 MHz, $CDCl_3$, δ ppm): 1.39 (d, J = 8.69 Hz, 3H), 2.04 (s, 3H), 3.48 (s, 1H), 3.71–3.81 (m, 1H), 4.08–4.15 (m, 1H), 6.66 (d, J = 15.36 Hz, 1H), 6.95 (s, 1H), 7.07 (t, J = 8.68 Hz, 2H), 7.45–7.49 (m, 2H), 7.64 (d, J = 15.18 Hz, 1H). ESI-MS: 334.1 ($C_{16}H_{17}FN_3O_4$, $[M+H]^+$). Anal. Calcd for $C_{16}H_{16}FN_3O_4$: C, 57.65; H, 4.84; N, 12.61. Found: C, 57.23; H, 5.01; N, 12.49.

4.3.10. (*E*)-1-(2-Methyl-5-nitro-1*H*-imidazol-1-yl)propan-2-yl 3-(4-chlorophenyl)acrylate (3j)

White powder, yield 56.1%, mp: 217–219 °C, ^{1}H NMR (300 MHz, $CDCl_3$, δ ppm): 1.43 (d, J = 8.23 Hz, 3H), 1.92 (s, 3H), 3.36 (s, 1H), 3.71–3.78 (m, 1H), 4.08–4.15 (m, 1H), 6.66 (d, J = 15.36 Hz, 1H), 6.84 (s, 1H), 7.35 (d, J = 8.58 Hz, 2H), 7.41 (d, J = 8.61 Hz, 2H), 7.62 (d, J = 15.39 Hz, 1H). ESI-MS: 350.1 ($C_{16}H_{17}ClN_3O_4$, $[M+H]^+$). Anal. Calcd for $C_{16}H_{16}ClN_3O_4$: C, 54.94; H, 4.61; N, 12.01. Found: C, 54.89; H, 4.81; N, 12.04.

4.3.11. (*E*)-1-(2-Methyl-5-nitro-1*H*-imidazol-1-yl)propan-2-yl 3-(4-bromophenyl)acrylate (3k)

White powder, yield 62.1%, mp: 220–222 °C, ^{1}H NMR (300 MHz, $CDCl_3$, δ ppm): 1.40 (d, J = 7.98 Hz, 3H), 2.05 (s, 3H), 3.74–3.76 (m, 1H), 4.08–4.13 (m, 2H), 6.54 (d, J = 15.00 Hz, 1H), 6.80 (s, 1H), 7.01–7.06 (m, 1H), 7.23–7.26 (m, 2H), 7.62 (d, J = 5.13 Hz, 1H), 7.80 (d, J = 15.00 Hz, 1H). ESI-MS: 394.0 ($C_{16}H_{17}BrN_3O_4$, $[M+H]^+$). Anal. Calcd for $C_{16}H_{16}BrN_3O_4$: C, 48.75; H, 4.09; N, 10.66. Found: C, 48.87; H, 4.31; N, 10.49.

4.3.12. (*E*)-1-(2-Methyl-5-nitro-1*H*-imidazol-1-yl)propan-2-yl 3-*p*-tolylacrylate (3l)

White powder, yield 62.9%, mp: 194–195 °C, ^{1}H NMR (300 MHz, $CDCl_3$, δ ppm): 1.42 (d, *J* = 8.12 Hz, 3H), 2.03 (s, 3H), 2.37 (s, 3H), 3.44–3.51 (m, 1H), 3.70–3.76 (m, 1H), 4.07–4.1 (m, 1H) 6.70 (d, *J* = 15.36 Hz, 1H), 7.08 (s, 1H), 7.18 (d, *J* = 7.89 Hz, 2H), 7.38 (d, *J*=8.22 Hz, 2H), 7.65 (d, *J* = 15.36 Hz, 1H). ESI-MS: 330.1 ($C_{17}H_{20}N_3O_4$, $[M+H]^+$). Anal. Calcd for $C_{17}H_{19}N_3O_4$: C, 62.00; H, 5.81; N, 12.76. Found: C, 61.87; H, 5.36; N, 12.49.

4.3.13. (*E*)-1-(2-Methyl-5-nitro-1*H*-imidazol-1-yl)propan-2-yl 3-(4-methoxyphenyl)acrylate (3m)

White powder, yield 67.8%, mp: 146–148 °C, ^{1}H NMR (300 MHz, $CDCl_3$, δ ppm): 1.41 (d, *J* = 6.79 Hz, 3H), 2.33 (s, 3H), 3.48 (s, 3H), 3.72–3.74 (m, 1H), 4.09–4.13 (m, 2H), 6.54 (d, *J* = 15.00 Hz, 1H), 6.80–6.91 (m, 1H), 7.01–7.06 (m, 1H), 7.23–7.26 (m, 2H), 7.35 (d, *J* = 5.13 Hz, 1H), 7.80 (d, *J* = 15.00 Hz, 1H). ESI-MS: 346.1 ($C_{17}H_{20}N_3O_5$, $[M+H]^+$). Anal. Calcd for $C_{17}H_{19}N_3O_5$: C, 59.12; H, 5.55; N, 12.17. Found: C, 59.31; H, 5.30; N, 11.79.

4.3.14. (*E*)-1-(2-Methyl-5-nitro-1*H*-imidazol-1-yl)propan-2-yl 3-(biphenyl-4-yl)acrylate (3n)

White powder, yield 58.7%, mp: 221–223 °C, ^{1}H NMR (300 MHz, $CDCl_3$, δ ppm): 1.42 (d, *J* = 7.99 Hz, 3H), 2.09 (s, 3H), 3.06 (s, 1H), 3.76–3.78 (m, 1H), 4.10–4.17 (m, 1H), 6.79 (d, *J* = 15.36 Hz, 1H), 7.03 (s, 1H), 7.35–7.39 (m, 1H), 7.46 (t, *J* = 7.41 Hz, 2H), 7.55–7.64 (m, 6H), 7.72 (d, *J* = 15.36 Hz, 1H). ESI-MS: 392.1 ($C_{22}H_{22}N_3O_4$, $[M+H]^+$). Anal. Calcd for $C_{22}H_{21}N_3O_4$: C, 67.51; H, 5.41; N, 10.74. Found: C, 67.31; H, 5.20; N, 10.99.

4.3.15. (*E*)-1-(2-Methyl-5-nitro-1*H*-imidazol-1-yl)propan-2-yl 3-(4-(benzyloxy)phenyl)acrylate (3o)

White powder, yield 53.36%, mp: 185–188 °C, ^{1}H NMR (300 MHz, $CDCl_3$, δ ppm): 1.40 (d, *J* = 8.05 Hz, 3H), 2.35 (s, 3H), 2.52 (s, 1H), 3.74–3.76 (m, 1H), 4.06–4.14 (m, 1H), 5.10 (s, 2H), 6.62 (d, *J* = 15.36 Hz, 1H), 6.91–7.00 (m, 2H), 7.13–7.15 (m, 1H), 7.31–7.45 (m, 7H), 7.64 (d, *J* = 15.36 Hz, 1H). ESI-MS: 422.2 ($C_{23}H_{24}N_3O_5$, $[M+H]^+$). Anal. Calcd for $C_{23}H_{23}N_3O_5$: C, 65.55; H, 5.50; N, 9.97. Found: C, 65.36; H, 5.78; N, 9.65.

4.3.16. (*E*)-1-(2-Methyl-5-nitro-1*H*-imidazol-1-yl)propan-2-yl 3-(4-(dimethylamino)phenyl)acrylate (3p)

Light grey powder, yield 57.1%, mp: 122–123 °C, ^{1}H NMR (300 MHz, $CDCl_3$, δ ppm): 1.40 (d, *J* = 3.84 Hz, 3H), 2.53 (s, 3H), 3.02 (s, 6H), 4.32–4.36 (m, 1H), 4.62–4.65 (m, 1H), 5.36 (t, *J* = 3.71 Hz, 1H), 6.04 (d, *J* = 9.42 Hz, 1H), 6.65 (d, *J* = *5.22* Hz, 2H), 7.37 (d, *J* = 5.22 Hz, 2H), 7.52 (d, *J* = 9.42 Hz, 1H), 7.92 (s, 1H). ESI-MS: 359.1 ($C_{18}H_{23}N_4O_4$, $[M+H]^+$). Anal. Calcd for $C_{18}H_{22}N_4O_4$: C, 60.32; H, 6.19; N, 15.63. Found: C, 60.54; H, 6.10; N, 15.39.

4.3.17. (*E*)-1-(2-Methyl-5-nitro-1*H*-imidazol-1-yl)propan-2-yl 3-(2,4-dichlorophenyl)acrylate (3q)

White powder, yield 56.9%, mp: 165–169 °C, ^{1}H NMR (300 MHz, $CDCl_3$, δ ppm): 1.43 (d, *J* = 8.44 Hz, 3H), 2.56 (s, 3H), 3.47–3.51 (m, 1H), 3.73–3.75 (m, 1H), 4.05–4.12 (m, 1H), 6.72 (d, *J* = 9.24 Hz, 1H), 6.96 (s, 1H), 7.23–7.26 (m, 1H), 7.40–7.46 (m, 2H), 7.94 (d, *J* = 9.24 Hz, 1H). ESI-MS: 384.0 ($C_{16}H_{16}Cl_2N_3O_4$, $[M+H]^+$). Anal. Calcd for $C_{16}H_{15}Cl_2N_3O_4$: C, 50.02; H, 3.94; N, 10.94. Found: C, 50.43; H, 4.10; N, 10.77.

4.3.18. (*E*)-1-(2-Methyl-5-nitro-1*H*-imidazol-1-yl)propan-2-yl 3-(naphthalen-1-yl)acrylate (3r)

White powder, yield 68.7%, mp: 176–179 °C, ^{1}H NMR (300 MHz, $CDCl_3$, δ ppm): 1.42 (d, *J* = 7.21 Hz, 3H), 2.12 (s, 3H), 3.72–3.81 (m, 2H), 4.11–4.20 (m, 1H), 6.83 (d, *J* = 15.18 Hz, 1H), 7.19 (s, 1H), 7.42–7.52 (m, 1H), 7.52–7.58 (m, 2H), 7.67 (d, *J* = 7.29 Hz, 1H), 7.87 (d, *J* = 7.50 Hz, 2H), 8.19 (d, *J* = 7.50 Hz, 1H), 8.51 (d, *J* = 15.18 Hz, 1H). ESI-MS: 366.1 ($C_{20}H_{20}N_3O_4$, $[M+H]^+$). Anal. Calcd for $C_{20}H_{19}N_3O_4$: C, 65.74; H, 5.24; N, 11.50. Found: C, 65.53; H, 5.37; N, 11.85.

4.3.19. (*E*)-1-(2-Methyl-5-nitro-1*H*-imidazol-1-yl)propan-2-yl 3-(naphthalen-2-yl)acrylate (3s)

White powder, yield 63.4%, mp: 204–206 °C, ^{1}H NMR (300 MHz, $CDCl_3$, δ ppm): 1.46 (d, *J*=9.04 Hz, 3H), 2.35 (s, 3H), 3.43–3.49 (m, 1H), 3.71–3.80 (m, 1H), 4.00–4.15 (m, 1H), 6.69 (s, 1H), 6.74 (s, 1H), 6.80–6.82 (m, 2H), 7.26 (s, 1H), 7.34 (d, *J* = 8.58 Hz, *2*H), 7.51 (d, *J* = 8.40 Hz, 2H), 7.60 (d, *J* = 15.36 Hz, 1H). ESI-MS: 366.1 ($C_{20}H_{20}N_3O_4$, $[M+H]^+$). Anal. Calcd for $C_{20}H_{19}N_3O_4$: C, 65.74; H, 5.24; N, 11.50. Found: C, 65.68%; H, 5.10; N, 11.97.

4.3.20. (*E*)-1-(2-Methyl-5-nitro-1*H*-imidazol-1-yl)propan-2-yl 3-(thiophen-2-yl)acrylate (3t)

Light grey powder, yield 72.9%, mp: 164–168 °C, ^{1}H NMR (300 MHz, $CDCl_3$, δ ppm): 1.40 (d, *J* = 6.79 Hz, 3H), 2.39 (s, 3H), 3.77–3.80 (m, 2H), 4.12–4.20 (m, 1H), 6.86 (d, *J* = 15.36 Hz, 1H), 6.96 (s, 1H), 7.50–7.53 (m, 1H), 7.60–7.63 (m, 1H), 7.81–7.87 (m, 1H), 7.91 (s, 1H). ESI-MS: 322.1 ($C_{14}H_{16}N_3O_4S$, $[M+H]^+$). Anal. Calcd for $C_{14}H_{15}N_3O_4S$: C, 52.33; H, 4.70; N, 13.08. Found: C, 51.96; H, 4.89; N, 12.83.

4.4. Antimicrobial activity

The antibacterial activity of the synthesized compounds was tested against *B. subtilis*, *E. coli*, *P. aeruginosa* and *S. aureus* using MH medium (Mueller–Hinton medium: casein hydrolysate 17.5 g, soluble starch 1.5 g, beef extract 1000 mL). The MICs (minimum inhibitory concentrations) of the test compounds were determined by a colorimetric method using the dye MTT (3-(4,5-dimethylth-iazol-2-yl)-2,5-diphenyl trtrazoliumbromide). A stock solution of the synthesized compound (100 μg/mL) in DMSO was prepared and graded quantities of the test compounds were incorporated in specified quantity of sterilized liquid MH medium. A specified quantity of the medium containing the compound was poured into microtitration plates. Suspension of the microorganism was prepared to contain approximately 10^5 cfu/mL and applied to microtitration plates with serially diluted compounds in DMSO to be tested and incubated at 37 °C for 24 h. After the MICs were visually determined on each of the microtitration plates, 50 μL of PBS (phosphate buffered saline 0.01 mol/L, pH 7.4, $Na_2HPO_4{\cdot}12H_2O$ 2.9 g, KH_2PO_4 0.2 g, NaCl 8.0 g, KCl 0.2 g, distilled water 1000 mL) containing 2 mg of MTT/mL was added to each well. Incubation was continued at room temperature for 4–5 h. The content of each well was removed, and 100 μL of isopropanol containing 5% 1 mol/L HCl was added to extract the dye. After 12 h of incubation at room temperature, the optical density (OD) was measured with a microplate reader at 550 nm. The observed MICs are presented in Table 2.

4.5. *E. coli* FabH purification and activity assay

Full-length *E. coli* acyl carrier protein (ACP), acyl carrier protein synthase (ACPS), and β-ketoacyl-ACP synthase III (FabH) were individually cloned into pET expression vectors with an N-terminal His-tag (ACP, ACPS in pET19; FabH in pET28).

All proteins were expressed in *E. coli* strain BL21 (DE3). Transformed cells were grown on Luria–Bertani (LB) agar plates supplemented with Kanamycin (30 μg/mL). Sodium dodecyl sulfatepolyacrylamide gel electrophoresis (SDS–PAGE) analysis was used to screen colonies for overexpression of proteins. One such positive colony was used to inoculate 10 mL of LB medium with 30 μg/mL of Kanamycin and grown over night at 37 °C, 1 mL of

which was used to inoculate 100 mL LB medium supplemented with 30 μg/mL of Kanamycin. The culture was shaken for 4 h at 37 °C, and then induced with 0.5 mM isopropyl β-D-thiogalactopyranoside (IPTG). The culture was grown for 4 h, and harvested by centrifugation (30 min at 15000 rpm).

Harvested cells containing His-tagged ACP, ACPS, and FabHs were lysed by sonication in 20 mM Tris, pH 7.6, 5 mM imidazole, 0.5 M NaCl and centrifuged at 20,000 rpm for 30 min. The supernatant was applied to a Ni-NTA agarose column, washed, and eluted using a 5–500 mM imidazole gradient over 20 column volumes. Eluted protein was dialyzed against 20 mM Tris, pH 7.6, 1 mM DTT, and 100 mM NaCl. Purified FabHs were concentrated up to 2 mg/mL and stored at −80 °C in 20 mM Tris, pH 7.6, 100 mM NaCl, 1 mM DTT, and 20% glycerol for enzymatic assays.

Purified ACP contains the apo-form that needs to be converted into the holo-form. The conversion reaction is catalyzed by ACP synthase (ACPS). In the final volume of 50 mL, 50 mg ACP, 50 mM Tris, 2 mM DTT, 10 mM $MgCl_2$, 600 μM CoA, and 0.2 μM ACPS was incubated for 1 h at 37 °C. The pH of the reaction was then adjusted to approximately 7.0 using 1 M potassium phosphate. Holo-ACP was purified by fractionation of the reaction mixture by Source Q-15 ion exchange chromatography using a 0–500 mM NaCl gradient over two column volumes.

In a final 20 μL reaction, 20 mM Na_2HPO_4/NaH_2PO_4, pH 7.0, 0.5 mM DTT, 0.25 mM $MgCl_2$, and 2.5 μM holo-ACP were mixed with 1 nM FabH, and H_2O was added to 15 μL. After 1 min incubation, a 2 μL mixture of 25 μM acetyl-CoA and 0.75 μCi [^{3}H] acetyl-CoA was added for FabH reaction for 25 min. The reaction was stopped by adding 20 μL of ice-cold 50% TCA, incubating for 5 min on ice, and centrifuging to pellet the protein. The pellet was washed with 10% ice-cold TCA and resuspended with 5 μL of 0.5 M NaOH. The incorporation of the ^{3}H signal in the final product was read by liquid scintillation. When determining the inhibition constant (IC_{50}), inhibitors were added from a concentrated DMSO stock such that the final concentration of DMSO did not exceed 2%.

4.6. Molecular docking modeling

The crystal structures of *E. coli* FabH (PDB code: 1HNJ)[21] was obtained from the Protein Data Bank (http://www.rcsb.org).

Studies were carried out on only one subunit of the enzymes. The graphical user interface AutoDockTools (ADT) was employed to setup the enzymes: all hydrogens were added, Gasteiger charges were calculated and nonpolar hydrogens were merged to carbon atoms. For macromolecules, generated pdbqt files were saved.

The 3D structures of ligand molecules were built, optimized (PM3) level, and saved in mol2 format with the aid of the molecular modeling program Spartan (Wavefunction Inc.). These partial charges of Mol2 files were further modified by using the ADT package (version1.4.6) so that the charges of the nonpolar hydrogens atoms assigned to the atom to which the hydrogen is attached. The resulting files were saved as pdbqt files.

AutoDock 4.0 was employed for all docking calculations.[22,23] The AutoDockTools program was used to generate the docking input files. In all docking a grid box size of 48 × 48 × 48 points in x, y, and z directions was built in the catalytic site of the protein. A grid spacing of 0.375 Å (approximately one forth of the length of carbon–carbon covalent bond) and a distances-dependent function of the dielectric constant were used for the calculation of the energetic map. Ten runs were generated by using Lamarckian genetic algorithm searches. Default settings were used with an initial population of 50 randomly placed individuals, a maximum number of 2.5 × 106 energy evaluations, and a maximum number of 2.7 × 104 generations. A mutation rate of 0.02 and a crossover rate of 0.8 were chosen. Results differing by less than 0.5 Å in positional root–mean–square deviation (RMSD) were clustered together and the results of the most favorable free energy of binding were selected as the resultant complex structures.

Acknowledgments

This work was supported by Jiangsu National Science Foundation (No. BK2009239) and the Fundamental Research Funds for the Central Universities (Nos. 1092020804 & 1106020824).

References and notes

1. Leeb, M. *Nature* **2004**, *431*, 892.
2. Lee, J.-Y.; Jeong, K.-W.; Lee, J.-U.; Kang, D.-I.; Kim, Y. *Bioorg. Med. Chem.* **2009**, *17*, 5408.
3. Lai, C. Y.; Cronan, J. E. *J. Biol. Chem.* **2003**, *19*, 51494.
4. Lu, Y. J.; Zhang, Y. M.; Rock, C. O. *Biochem. Cell Biol.* **2004**, *82*, 145.
5. Lv, P. C.; Sun, J.; Luo, Y.; Yang, Y.; Zhu, H. L. *Bioorg. Med. Chem.* **2010**, *20*, 4657.
6. Li, H. Q.; Luo, Y.; Lv, P. C.; Shi, L.; Liu, C. H.; Zhu, H. L. *Bioorg. Med. Chem. Lett.* **2010**, *20*, 2025.
7. White, S. W.; Zheng, J.; Zhang, Y. M.; Rock, C. O. *Annu. Rev. Biochem.* **2005**, *74*, 791.
8. Asheka, A.; Cho, S. J. *Bioorg. Med. Chem.* **2006**, *14*, 1474.
9. (a) Lau, N. P.; Piscitelli, S. C.; Wilkes, L.; Danziger, L. H. *Clin. Pharmacokinet.* **1992**, *23*, 328; (b) Uto, Y.; Nagasawa, H.; Jin, C. Z.; Nakayama, S.; Tanaka, A.; Kiyoi, S.; Nakashima, H.; Shimamura, M.; Inayama, S.; Fujiwara, T.; Takeuchi, Y.; Uehara, Y.; Kirk, K. L.; Nakata, E.; Hori, H. *Bioorg. Med. Chem.* **2008**, *16*, 6042.
10. Lord, E. M.; Harwell, L.; Koch, C. J. *Cancer Res.* **1993**, *53*, 5721.
11. *Martindale the Extra Pharmacopoeia*, 27ed., The Pharmaceutical Press, London, 1977, p 1570.
12. Boza, A.; Gonzalez, R.; Novoa, H.; Cuéllar, D. M.; Valdés, M. *IL Farmaco.* **2000**, *55*, 700.
13. Gillis, J. C.; Wiseman, L. R. *Drugs* **1996**, *51*, 621.
14. Soedin, K.; Syukran, O.; Fadillah, A.; Sidabutar, P. *Pharmaceutica* **1985**, *4*, 251.
15. Wang, Z.-M.; Kolb, H. C.; Sharpless, K. B. *J. Org. Chem.* **1994**, *59*, 5104.
16. Meydan, N.; Grunberger, T.; Dadi, H.; Shahar, M.; Arpaia, E.; Lapidot, Z.; Leeder, J. S.; Freedman, M.; Cohen, A.; Gazit, A.; Levitzki, A.; Roifman, C. M. *Nature* **1996**, *379*, 645.
17. Molinos, Antonio Cobo; Abriouel, Hikmate; López, Rosario Lucas; Omar, Nabil Ben; Valdivia, Eva; Gálvez, A. *Food Microbiol.* **2008**, *25*, 762.
18. Silici, S.; Ünlü, M.; Vardar-Ünlü, G. *World J. Microbiol. Biotechnol.* **2007**, *23*, 1797.
19. Qian, Y.; Zhang, H. J.; Zhang, H.; Xu, C.; Zhao, J.; Zhu, H. L. *Bioorg. Med. Chem.* **2010**, *18*, 4991.
20. Davis, R.; Kumar, N. S.; Abraham, S.; Suresh, C. H.; Rath, N. P.; Tamaoki, N.; Das, S. *J. Phys. Chem.* **2008**, *112*, 2137.
21. Qiu, X.; Janson, C. A.; Smith, W. W.; Head, M.; Lonsdale, J.; Konstantinidis, A. K. *J. Mol. Biol.* **2001**, *307*, 341.
22. Morris, G. M.; Goodsell, D. S.; Halliday, R. S.; Huey, R.; Hart, W. E.; Belew, R. K.; Olson, A. J. *J. Comput. Chem.* **1998**, *19*, 1639.
23. Huey, R.; Morris, G. M.; Olson, A. J.; Goodsell, D. S. *J. Comput. Chem.* **2007**, *28*, 1145.